Bulletin of Earthquake Engineering
https://doi.org/10.1007/s10518-024-01956-3

ORIGINAL ARTICLE

Assessing the impact of the 2023 Kahramanmaraş and Hatay earthquakes on cadastre and property data using GPS and GIS

Emre Ayso[1] · İrem Köz[1] · Serkan Doğanalp[1] · Mustafa Aslan[2] · Ekrem Tuşat[1] · Muzaffer Kahveci[1] · Cahit Taşpınar[3]

Received: 19 January 2024 / Accepted: 10 June 2024
© The Author(s) 2024

Abstract
Natural disasters such as earthquakes, storms, floods, landslides, and tsunamis cause significant losses in land and buildings, which are an integral part of human life. This causes inconsistency between the actual situation in the land and official records and brings legal problems with it. In other words, natural disasters negatively affect human life and cause problems in the country's cadastral system and land ownership and usage. Therefore, after natural disasters, rapid and fair redefinition of cadastral works and land boundaries in the affected areas is an important need of the society and is the basis of trust in the state. In this study, the effects of the 06 February 2023 (Mw = 7.7, Mw = 7.6) Kahramanmaraş and 20 February 2023 (Mw = 6.4) Hatay earthquakes on the cadastral status of the parcels in and around Kırıkhan district of Hatay province were investigated. By modeling the displacements, the deformation sizes of 4044 parcel corner coordinates and 1333 parcel areas were calculated and analyzed. In terms of the protection of property rights in land management, some suggestions were made by presenting concrete findings of coordinate and areal changes.

Keywords ANFIS · Cadastre · Displacement · Earthquake · GIS · GPS

1 Introduction

An earthquake is a violent shaking of the earth's surface caused by the propagation of seismic waves as a result of breaks in the earth's crust (sudden energy release) or volcanic movements. Hence, it can be said that earthquake is a seismic activity on Earth. The asthenosphere, zone of Earth's mantle that separates the relatively rigid lithosphere from the deeper mantle and believed to be more fluid than the lithosphere (Hua et al. 2023). Movements on faults formed at tectonic plate boundaries or weak points of these plates cause earthquakes. Three major earthquake zones of the earth have been defined. These are the circum-Pacific seismic belt, the Alpide earthquake belt and the Mid-Atlantic ridge (USGS 2023a). Biggest earthquakes in recorded history have occurred in the circum-Pacific seismic belt such as the Chilean Earthquake (1960, Mw ~ 9.5), the (1964, Mw ~

Extended author information available on the last page of the article

Published online: 15 June 2024

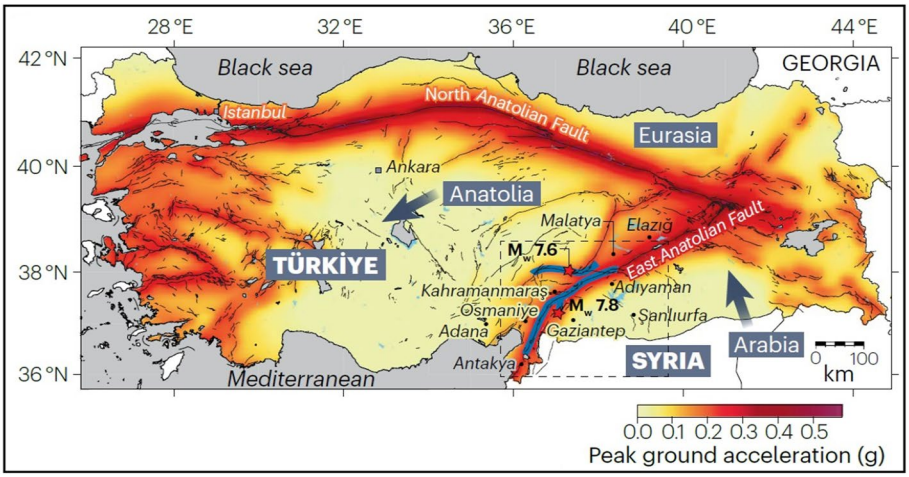


Fig. 1 Seismic hazard and tectonic map of Türkiye (AFAD 2023a; Hussain et al. 2023)

9.2) and the Indian Ocean Earthquake (2004, Mw ~ 9.0), (Pal et al. 2023). About 90% of the world's earthquakes occur here. The next most seismic region is the Alpine belt stretching eastward from the Mediterranean region over Türkiye, Iran, and Northern India, where about 5–6% of earthquakes occur (USGS 2023b). A significant part of Türkiye is located in the Alpine-Himalayan seismic belt. Earthquakes in Türkiye are mostly tectonic earthquakes caused by plate movements. Tectonically, Türkiye has a highly active structure due to the many faults it contains. Türkiye, which is mainly under the influence of the Eurasian, African and Arabian plates, is in the Alpine Himalayan seismic belt stretching from Gibraltar to the Indonesian islands. The Anatolian block has moved to W–SW due to the movement of African plate towards Eurasian plate (Kahveci et al. 2019). Figure 1 depicts a map of Türkiye's earthquake risk and regional plate tectonics developed by Disaster and Emergency Management Presidency in Türkiye (AFAD 2023a) and Hussain et al. 2023.

According to Kurt et al. (2022), based on the improved coverage of velocity field of Türkiye, obtained from a GNSS (Global Navigation Satellite Systems) campaign period of up to 28 years at 836 stations, modelled slip rates vary between 20 and 26 mm/yr and 9.7 and 11 mm/yr for the North and East Anatolian faults, respectively (Fig. 2). Thousands of earthquakes have occurred due to active faults in Türkiye. The distribution of earthquakes with Mw ≥ 5 from 01.01.1900 to 07.08.2023 is given in Fig. 3.

In Türkiye, 11 cities (approximately 14 million people) were affected by the earthquakes that took place in Kahramanmaraş on February 06, 2023, and in Hatay on February 20, 2023, resulting in significant loss of life and property (Anadolu Ajansı 2023; T.C. S.B.B. 2023). In addition to all these negative results, these earthquakes also caused the information such as coordinates and parcel areas of the region in the Türkiye cadastral system to change. This changed information should be updated in the country's land register system, eliminating the effects of deformation caused by earthquakes and protecting the rights of real estate. As it is known, a land register is a formal record maintained by government authorities that contains comprehensive details about land ownership, boundaries, and other legal rights associated with land parcels within a specific jurisdiction. Thus, the property ownership is constitutionally guaranteed in Türkiye. Article 35 of the 1982 Constitution of Türkiye, which regulates the right to property, contains

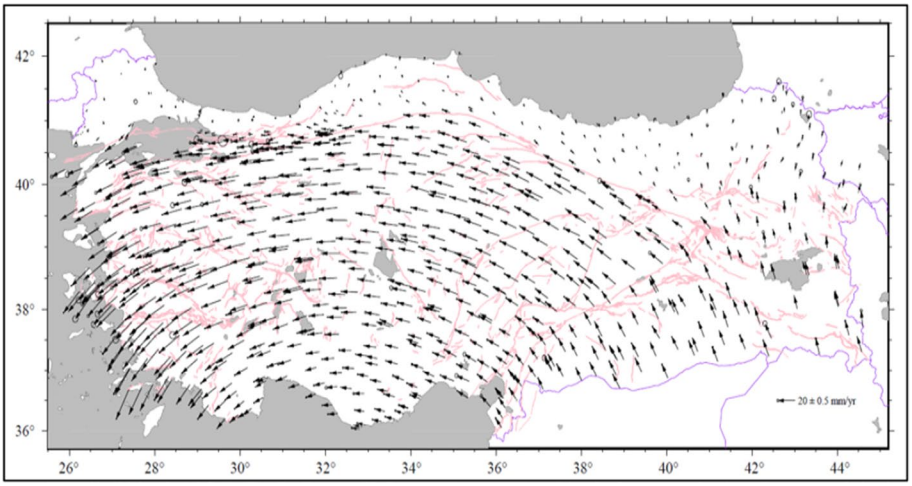


Fig. 2 The velocity solution of Türkiye in the Eurasia-fixed reference frame (Kurt et al. 2022)

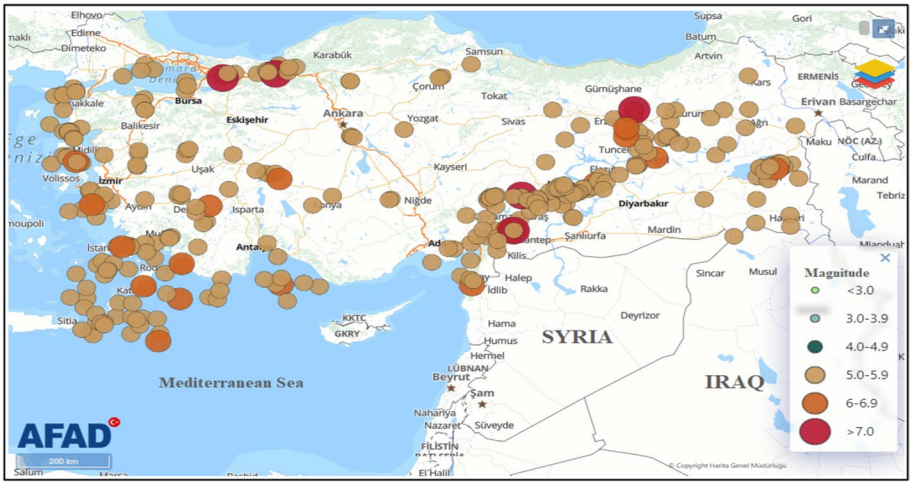


Fig. 3 Distribution of earthquakes with Mw ≥ 5 between 1900 and 2023 in Türkiye (AFAD 2023b)

the following provision: "Everyone has property and inheritance rights. These rights can only be limited by law for the public interest. The use of the right to property can not be contrary to public interest." (T.R. Constitution 1982).

On the other hand, tectonic activities on the plates; It has become a research topic in many fields such as earthquake, climate change, geodynamics and geodesy, and its effects on reference system definitions (Altamimi et al. 2017; Hay 1996; Jagoda 2021; Ramstein et al. 2019). Koyanagi et al. (2020) examined the features of landslides in grasslands and forests that were caused by the Mw 7.0 Kumamoto earthquake in 2016 in order to clarify the impact of land cover on landslides that are caused by earthquakes. Kincey et al. (2023)

investigated the landslides that occurred within 4.5 years after the Mw 7.8 earthquake in Gorkha/Nepal in 2015. And they have found that 14% (85 km^2) of the total modelled potential runout area experienced landslide activity within 4.5 years after the earthquake. Grant et al. (2014) stated that a sequence of earthquakes occurred in 2010 and 2011 in the Canterbury region of New Zealand caused widespread damage and resulted in some cadastral boundaries being ruptured by up to 4 m. And in line with the "dynamic cadastre" proposal made in 1995, a local deformation model was developed to model the seismic movements. Park et al. (2019) examines the conceptual link between disaster management and land administration. The real estate market and the danger zone were also explored in terms of land tenure, value, usage, and development. In Mitchell et al. (2017), the challenges in land management after the earthquakes in Haiti, Nepal and New Zealand are stated, regulatory policies for land management, institutional, operational, and preparatory stages are discussed, and a framework for evaluating the earthquake-responsiveness of a land administration system was proposed.

In this study, the effects of the 06 February 2023 (Mw = 7.7, Mw = 7.6) Kahramanmaraş and 20 February 2023 (Mw = 6.4) Hatay earthquakes on the cadastral parcels in and around the Kırıkhan district of Hatay province were investigated.

2 Kahramanmaraş (6 february 2023) and hatay (20 february 2023) earthquakes

Many scientific studies have been carried out about Kahramanmaraş province and its surroundings, which are under the influence of the Eastern Anatolia and Dead Sea active faults. And it has been known long since that the region is one of the high-risk areas due to the continuous accumulation of energy and the presence of seismic gaps in the faults, (Biricik and Korkmaz 2001; Kop et al. 2014; Sünbül and Sünbül 2017). An earthquake occurred in Pazarcık (Kahramanmaraş) on 06 February 2023 at 04:17 local time (Mw = 7.7, focal depth 8.6 km) and approximately 9 h after this earthquake, a second earthquake occurred in Elbistan (Kahramanmaraş) at 13:24 local time (Mw = 7.6 and focal depth of 7.0 km) (AFAD 2023c). Considering the earthquake depths, both earthquakes can be said to be shallow earthquakes. While the effects of the first two earthquakes continued, Türkiye was shaken once again by a third earthquake. On February 20, 2023, at 20:04 local time, a third earthquake with a moment magnitude of 6.4 and a focal depth of 21.7 km occurred in Yayladağı (Hatay) (AFAD 2023d). Summary information about the earthquakes in question is shown in Table 1. The epicenters of the earthquakes are shown in Fig. 4 prepared using QGIS.org (2023) software.

The effects of these earthquakes were felt strongly in many provinces and caused heavy loss of life and property. A state of emergency was declared for the provinces of Kahramanmaraş, Gaziantep, Şanlıurfa, Adıyaman, Hatay, Osmaniye, Adana, Malatya, Diyarbakır, Kilis and Elazığ, which were declared earthquake zones. According to the 2022 ABPRS (Address Based Population Registration System) data, the population in these 11 provinces most affected by the earthquake is 14,012,196. As a result of the earthquakes, more than 50 thousand people lost their lives, and more than 107 thousand people were injured (Anadolu Ajansı 2023; T.C. S.B.B. 2023). It has been stated that the impact of earthquakes on the Turkish economy is approximately 2 trillion TL (103.6 billion USD), and this amount can reach approximately 9% of the national income in 2023. As of March 6, 2023, damage assessment studies were carried out for

Table 1 Information about the earthquakes (AFAD 2023c, AFAD 2023d)

Location	Date and time	Moment magnitude (Mw)	Depth of focus (km)
Pazarcık/Kahramanmaraş 37.288°N and 37.043°E	06.02.2023 01:17:34 UTC	7.7	8.6
Elbistan/Kahramanmaraş 38.089°N and 37.239°E	06.02.2023 10:24:47 UTC	7.6	7.0
Yayladağı/Hatay 36.037°N and 36.021°E	20.02.2023 17:04:27 UTC	6.4	21.7

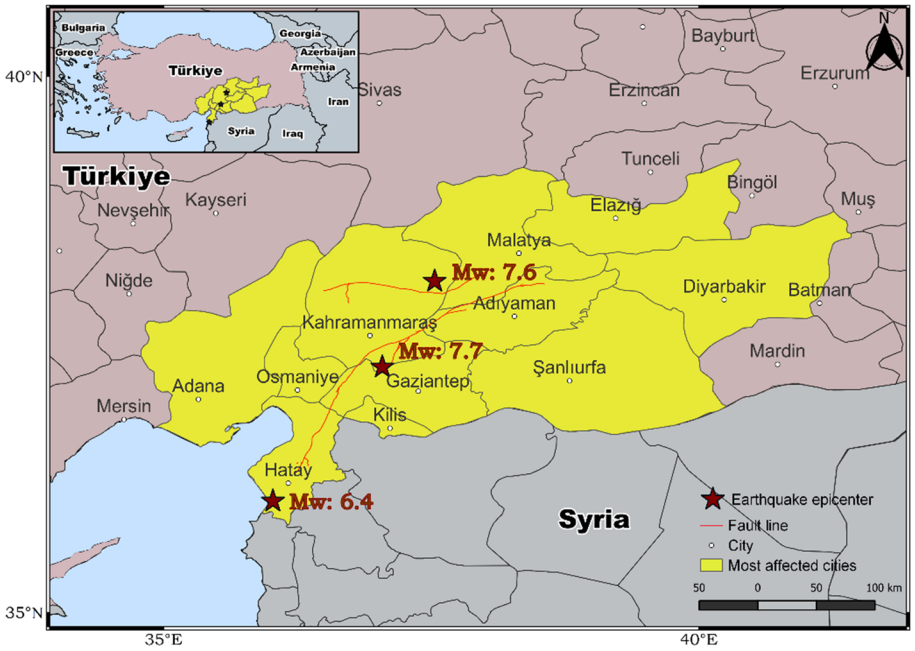


Fig. 4 Epicenters of Kahramanmaraş and Hatay earthquakes

1,712,182 buildings in 11 provinces affected by the earthquake. It was announced that 35,355 buildings were destroyed, 17,491 buildings needed to be demolished urgently, 179,786 buildings were heavily damaged, 40,228 buildings were moderately damaged, and 431,421 buildings were slightly damaged. Among the destroyed or severely damaged buildings, there are historical and cultural buildings, schools, administrative buildings, hospitals, hotels as well as those used as residences (T.C. S.B.B. 2023). There are 5,378,280 parcels in total in 11 provinces declared as earthquake zones (Aslan 2023). In some sources, it is stated that structures built before 2000 were greatly affected by earthquakes (Sagbas et al. 2024). The reason for this is that most of the buildings that caused loss of life were not built in accordance with the relevant legislation and did not meet the minimum requirements of the seismic design regulations of the period (Aydogdu and Ilki 2024).

The Pazarcık (Kahramanmaraş) earthquake with a magnitude of Mw 7.7 occurred in the Narlı segment at the northern end of the left-lateral Dead Sea Fault Zone. The Mw 7.6 Elbistan (Kahramanmaraş) earthquake occurred on the Çardak Fault, which is a

branch of the East Anatolian Fault (AFAD 2023c). After these two major earthquakes, the Yayladağı (Hatay) earthquake of Mw 6.4 took place (AFAD 2023d). After these earthquakes, intense aftershocks occurred. 12,288 earthquakes occurred in Türkiye from 01.02.2023 to 28.02.2023 (BOUN KOERI RETMC 2023).

3 Cadastre, property and earthquake relations

The relationship between people and land has always remained dynamic from primitive societies to the present. This dynamic structure, within the scope of human activities on the land, has developed in the form of benefiting, using, sheltering, owning, and seeing the land as an investment total Population growth, economic growth and scarcity of land resources have forced countries to regulate people's relationships with their land. The cadastre, which emerged as systems regulating human-land relations, was defined by Dale and McLaughlin (1988) as "an official record of information about parcels of land, including details of their boundaries, tenure, use, and value". FIG (1995) defined the cadastre as "a parcel-based and up-to-date land information system that includes a record of interests in the land (e.g., rights, restrictions and responsibilities)''. Based on these definitions, cadastral data include information about the owner, types of rights, area, boundaries of parcels, and unique identification number that can be linked to other land-related information, which are basic information about people's relationship with their land. Thanks to these data, the relationship between people and land has become more dynamic.

Within the scope of cadastral activities, the locations and owners of each immovable and the independent sections on it are determined. Keeping this information up-to-date is of vital importance for the protection of property rights, new constructions, and the resolution of disputes. It is clear that a healthy property data will be needed in many activities, from debris removal after large-scale devastating earthquakes to identifying new residential areas. The importance of determining the property data needed from the first moment of earthquakes and the situation after the earthquake emerges here. Reliable and up-to-date cadastral data and location-based data on land objects, providing a platform for the implementation of decisive action before, during and after a disaster (Barra et al. 2020).

All disasters, especially earthquakes, are much more destructive for both vital and physical superstructure and infrastructure, and also cause major problems on geodetic networks and "cadastral borders" that constitute the infrastructure of property rights.

The effect of ground movements that occur as a result of the earthquake and affect the cadastral boundaries on the property boundaries can be determined more clearly by performing the following actions (Grant and Crook 2012):

a. Direct observation of displacements along fault rupture,
b. Renewal of measurements at GNSS points,
c. Comparison of satellite-based images before and after the earthquake,
d. Reproduction of precision orthophoto maps.

4 Material and methods

In this study, an application was carried out in and around the borders of Kırıkhan district of Hatay province in Türkiye, which were affected by the 06 February 2023 (Mw = 7.7, Mw = 7.6) Kahramanmaraş and 20 February 2023 (Mw = 6.4) Hatay earthquakes. With this application, areal and coordinate changes due to occurred earthquakes in cadastral and property data were examined. The data used to model displacements in the study area are static and RTK (Real-Time Kinematics) data obtained before earthquakes. The static measurement method is the classical GPS measurement technique and is best for applications where very high accuracy is required, such as the determination of crustal or plate movements, for long baselines, when the available satellite geometry does not allow for any other measurement technique, and when systematic effects (e.g. ionosphere, troposphere) must be taken into account. In this method, simultaneous measurements are made with two or more receivers for at least one hour (Kahveci and Yıldız 2022). In addition, point positions and detail points need to be established in real time in engineering applications. The classical RTK approach was created for this reason, and it provides real-time point position determination in centimeter level. Coordinates before earthquakes, connected to TNFGN (Turkish National Fundamental GPS Network), were produced in cadastral works by different institutions, then checked and archived by the General Directorate of Land Registry and Cadastre (GDLRC). The points mentioned (C3 order, detail and polygon (C4 order) points) were produced in accordance with the Large-Scale Map and Map Information Production Regulation of Türkiye (BÖHHBÜY 2005, 2018). Accordingly, in static method, the horizontal accuracy limit for C3 order points is given as ± 5 cm, the vertical accuracy limit is given as ± 6 cm. For detail points, horizontal and vertical accuracy limits are both given as ± 7 cm, and for polygon points, horizontal and vertical accuracy limits are given as ± 8 cm. Therefore, the lowest accuracy of archive coordinates is ± 8 cm, which is within the error limits of this study.

The coordinates C3 order points, polygon and detail points were obtained using Network-RTK method, which was carried out between 23–25 February 2023, after earthquakes. They were obtained with a study led by one of the authors conducted in GDLRC. With the Network-RTK method, observations connected to the CORS-TR (Continuously Operating Reference Stations-Türkiye) network were carried out. At each station, two measurements were performed one hour apart, and the average of the obtained coordinates was utilized. Horizontal position accuracies are better than ± 7 cm as expected from RTK-GPS. Briefly, before and after earthquakes obtained coordinate accuracies of all GPS measurements are better than ± 8 cm. The point coordinates used in the study are in the TNRF (Türkiye National Reference Frame) and the plane coordinates of the points mentioned are in the TM (Transversal Mercator) projection system (as N: Northing; E: Easting). TNRF represents a 4-dimensional national datum within the ITRF96 (2005.0 epoch) datum, which was created by connecting to the TNFGN and CORS-TR (TUSAGA-Active) networks. The distribution of points (as training and test points) and fault lines in the study area are shown in Fig. 5 prepared in ArcMap software developed by ESRI® (2023). The training points in question are the points used for training the artificial neural network, and the test points are the points used for testing the model created with the neural networks.

In order to determine the changes in cadastral and property data after earthquakes, it is aimed to determine the most appropriate model for the study area. In this context, Adaptive Network Based Fuzzy Inference Systems (ANFIS) (Jang 1993) was used for the model. ANFIS architecture is known as a hybrid method developed by Zadeh

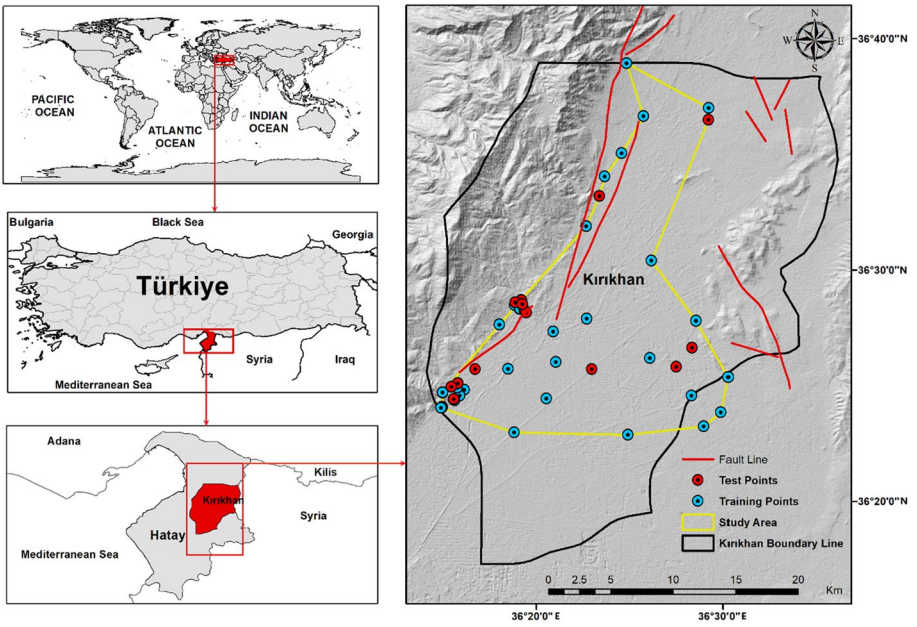


Fig. 5 Study area, distribution of points and fault lines

(1965). Fuzzy rules created with ANFIS are created with Sugeno type fuzzy model. This model enables fuzzy systems to learn parameters adaptively. The Sugeno fuzzy model (TSK: Takagi–Sugeno-Kang fuzzy model) is proposed to develop a systematic approach to generate fuzzy rules from a given input–output data set (Sugeno and Kang 1988; Takagi and Sugeno 1985). For a first-order Sugeno fuzzy model with two inputs (x, y) and one output (z), the two fuzzy if–then rules can be written as in Eq. 1 and 2 (Jang and Sun 1995).

Rule 1: If x is A_1 and y is B_1, then $f_1 = p_1x + q_1y + r_1$ (1)

Rule 2: If x is A_2 and y is B_2, then $f_2 = p_2x + q_2y + r_2$ (2)

In the fuzzy rules in Eqs. 1, 2, while the "if" part has a fuzzy structure, the "then" part expresses a definite function. In other words, the expressions A_i and B_i in the antecedent (relating to x and y, respectively) represent fuzzy sets, the resultant f_i represents a clarified real function. Finally, p_i, q_i and r_i expressions represent the design parameters during ANFIS training.

Figure 6 explains the working principle of the ANFIS architecture. The neuro-fuzzy model presented here includes a five-layer network to implement a Sugeno-type fuzzy system. These are (Karaboga and Kaya 2019);

Layer 1: It is defined as a fuzzification layer that uses membership functions to obtain fuzzy sets from input parameters.

Layer 2: It is defined as the rule layer responsible for generating the firing strengths (w_i) for the rules.

Layer 3: This layer, known as the normalization layer, calculates the normalized firing powers for each rule.

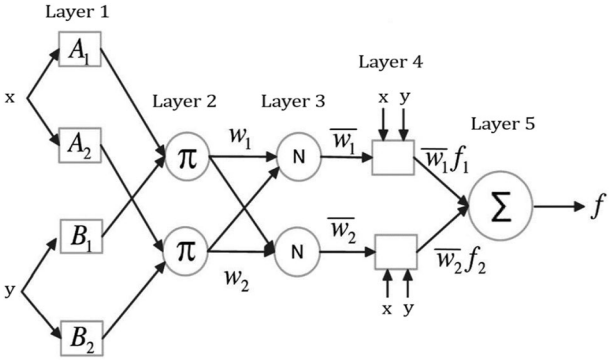


Fig. 6 ANFIS architecture for a first-order two-input Sugeno type fuzzy model

Layer 4: This layer is called the defuzzification layer. Normalized values are defuzzificated in this layer and prepared for transfer to the last layer.
Layer 5: This last layer, called the summation layer, produces the actual outputs.

From this point of view, Neuro-Fuzzy Designer interface was used on the MATLAB® platform produced by The MathWorks Inc (2020) to create the model and test the accuracy of the model. Of the 71 points obtained in the study area, 53 were used as training points and 18 as test points. In other words, 75% of the data used for the development of the model is reserved for training and 25% for testing (Fig. 5). In the ANFIS architecture, the $N_{BE}\left(N_{\text{BeforeEarthquake}}\right)$ and $E_{BE}\left(E_{\text{BeforeEarthquake}}\right)$ projection coordinates of the points before the earthquake represent the input parameters of the system. The difference in the projection coordinates (dN, dE) of the points after the earthquake $N_{AE}\left(N_{\text{AfterEarthquake}}\right)$, $E_{AE}\left(E_{\text{AfterEarthquake}}\right)$ and before the earthquake $\left(N_{BE}, E_{BE}\right)$ represents the output parameters (Eqs. 3, 4):

$$dN = N_{AE} - N_{BE} \tag{3}$$

$$dE = E_{AE} - E_{BE} \tag{4}$$

Therefore, the ANFIS architecture is built on 2 different scenarios; 2 inputs $\left(N_{BE}, E_{BE}\right)$, 1 output (dN) and 2 inputs $\left(N_{BE}, E_{BE}\right)$, 1 output (dE). Thus, separate models have been developed for displacements dN in the Northing direction and dE in the Easting direction. Other important factors for establishing the model and training the network are to determine how many subsets the input parameters will be divided into and what kind of membership function (triangle, trapezoidal, gaussian, sigmoidal etc.) they will be used with. In order to find the most suitable model for different membership functions and training the network, the processes were repeated until the model with the lowest standard deviation and highest correlation value was found. In this context, according to many experimental tests with different subset numbers and membership functions, it has been seen that the most appropriate number of subsets for the dN component scenario is 5 for the N and E values, and for the dE component scenario N and E values are 5 and 6, respectively.

On the other hand, it has been seen that the most suitable membership functions for the dN and dE component scenarios are sigmoid (sigmf) and gaussian (gauss2mf),

respectively. The mathematical models of the sigmoid and gaussian membership functions are given in Eqs. 5, 6, respectively.

$$sigmoid(x;\mathrm{a},c) = \frac{1}{1+\exp[-a(x-c)]} \tag{5}$$

$$gaussian(x;\sigma,c) = e^{\left\{-\left[\frac{x-c}{\sigma}\right]^2\right\}} \tag{6}$$

Membership function parameters specified as a and c in Eq. (5) represent the slope and cross-over point, and membership function parameters specified as σ and c in Eq. 6 represent the center and width of the membership function, respectively (Jang and Sun 1995). ANFIS model structures related to the modeling in question are given in Figs. 7, 8.

When more than one model is considered, different statistical criteria can be used in the selection of the most suitable model. In this study, 10 different criteria (maximum, minimum, mean, median, R^2, d, c, AIC, RMS, STD) were considered and the most suitable model was selected according to these criteria. Three of these criteria's evaluation were explained below as an example.

- The Index of agreement (d) value ranges from 0 to 1, while a value of 1 indicates perfect agreement between observed and predicted observations, while a value of 0, on the contrary, indicates inconsistency.
- The confidence index (c) value greater than 0.85 is considered to be the best performance and less than 0.40 is considered to be the worst performance.

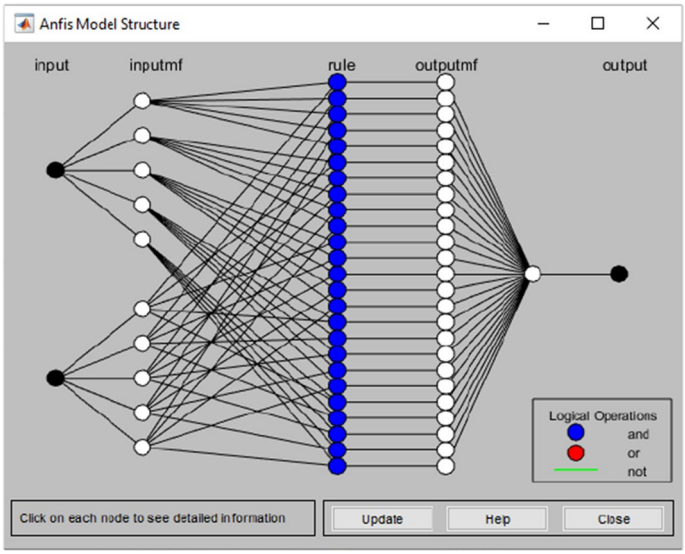


Fig. 7 Two-input ANFIS model structure for dN

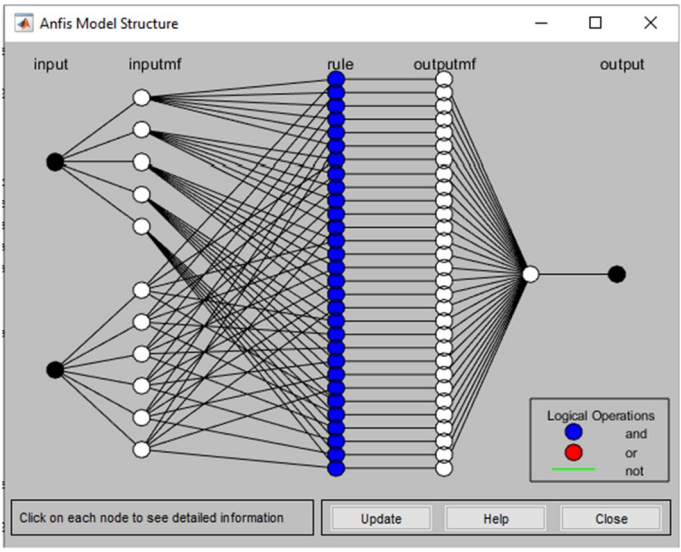


Fig. 8 Two-input ANFIS model structure for *dE*

- The smaller Akaike information criterion (AIC) value in model comparisons, the more suitable the model is. On the other hand, it is known that generally negative AIC values will be obtained by calculating AIC from regression statistics.

More detailed information about these criteria can be accessed from sources (Akaike 1973; Willmott 1981; Camargo and Sentelhas 1997; Anderson et al. 2004; Tusat and Mikailsoy 2018; Cavanaugh and Neath 2019).

5 Results and discussions

In this study, displacements related to the study area were modeled by applying the data and selection criteria explained in the material and method section. Using the model obtained, the changes in the cadastral and property data due to the earthquake were determined. Statistical information about the model obtained in this context is given in Table 2.

When the values in Table 2 are examined, it can be seen that the R^2 is very close to 1, standard deviation values are consistent with the accuracy of the used data (± 10 cm) and the mean and the median values are very close to zero. Accordingly, it can be said that the model formed is adequate from the statistical parameters point of view. With the created model, the displacement model was applied by using the parcel corner coordinates before the earthquakes in the study area, and the obtained output parameters (dN, dE) were added to the parcel corner coordinates before the earthquake and the post-earthquake parcel corner coordinates were predicted. Thus, the pre-earthquake $F_{BE}\left(F_{BeforeEarthquake}\right)$ and post-earthquake $F_{AE}\left(F_{AfterEarthquake}\right)$ areas of 1333 parcels were determined. The area changes in these parcels (dF) were obtained using Eq. 7, and their percentage ($dF\%$) equivalents were obtained using Eq. 8:

Table 2 Statistical information about the modelling

Statistics on modelling				
Criteria	Anfis training $dE(m)$	Anfis test dN (m)	dE (m)	dN (m)
Maximum	0.3755	0.4059	0.1975	0.3036
Minimum	−0.2924	−0.2375	−0.1251	−0.1985
Mean	0.0000	0.0000	0.0002	0.0075
Median	0.0000	−0.0001	−0.0291	−0.0096
R^2	0.9638	0.9966	0.9892	0.9977
d	0.9071	0.9962	0.9415	0.9978
c	0.8906	0.9945	0.9364	0.9967
AIC	−4.5074	−4.8123	−4.4259	−3.7098
RMSE	0.1019	0.0875	0.0993	0.1421
STD	0.1019	0.0875	0.0993	0.1419

$$dF = F_{AE} - F_{BE} \tag{7}$$

$$dF\% = \frac{dF}{F_{AE}} \tag{8}$$

In addition to this, changes in the corner coordinates of 4044 parcels (dN, dE) were also obtained and these changes are given in Tables 3 and 4. The parcels in question in the study area are shown in Fig. 9 prepared in the ArcMap software developed by ESRI® (2023).

As can be seen from Table 3, although the maximum change in the areas of the parcel is 30.806 m^2, the average amount of area change in all parcels is found to be 0.102 m^2. In terms of rate of change, this value corresponds to 0.001%. Morever, 99.40% of the changes in parcel areas due to the earthquake are smaller than 1 m^2 ($dF < 1m^2$). This amount of

Table 3 Area changes (m^2), 1333 units

Criteria	$dF(m^2)$	Absolute difference of area $\lvert dF\rvert(m^2)$	Rate of change $(dF\%)$
Maximum	30.806	30.806	0.357
Minimum	−23.216	0.0002	0.000
Mean	0.024	0.102	0.001
Median	0.025	0.026	0.000
STD	1.152	1.148	0.011

Table 4 Coordinates changes (m), 4044 units

Criteria	dE(m)	dN(m)	$\lvert dE\rvert$(m)	$\lvert dN\rvert$(m)
Maximum	0.498	2.015	0.498	2.015
Minimum	−0.134	−1.324	0.004	0.056
Mean	0.473	1.514	0.473	1.519
Median	0.478	1.543	0.478	1.543
STD	0.040	0.194	0.037	0.144

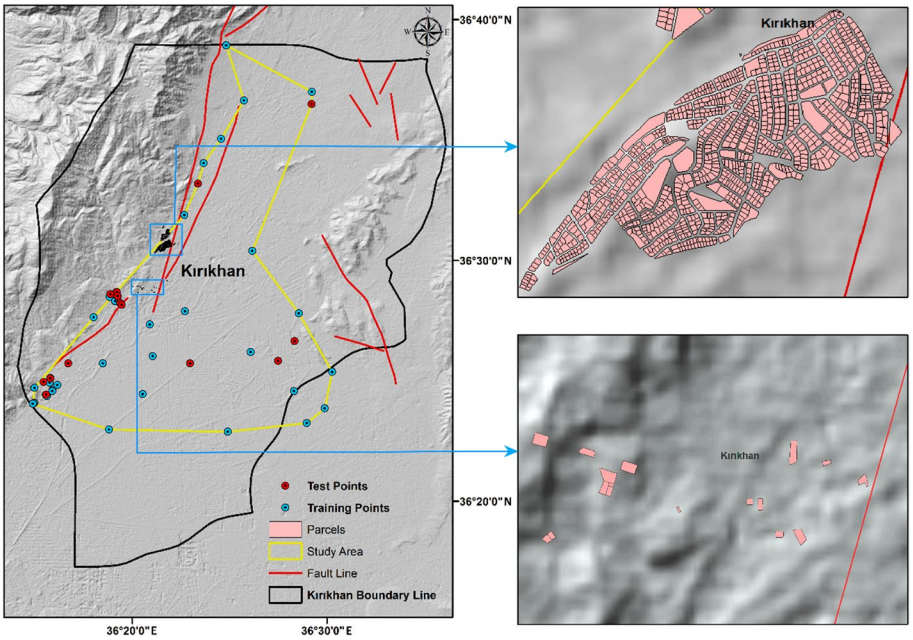


Fig. 9 Display of parcels in the study area

change is within the area allowance limit specified in the relevant regulations in Türkiye. In addition, when the changes in the corner coordinates of the parcel due to the earthquake, given in Table 4, are examined; maximum value in the E (East) direction is 0.498 m and in the N (North) direction is 2.015 m in absolute sense. Again, the mean absolute displacements in the parcel corner coordinates are 0.473 m in the E and 1.519 m in the N directions.

When the results of these two tables are evaluated together, the areas before and after the earthquake do not show much difference in terms of area. However, it is seen that the corner coordinates have changed significantly. Therefore, when examining the effects of earthquakes on cadastral parcels, it is considered that it would be an appropriate method to consider coordinate changes instead of area changes. On the other hand, in practice, official tolerance equations are used for area differences in title deeds in Türkiye. For example, parcel area tolerances for rural areas are calculated with Eq. 9 (GDLRC 2012; Ercan 2023).

$$df_{max} = 0.0004M\sqrt{F} + 0.0003F \tag{9}$$

Here, M is the scale denominator of the plan that covers the parcel, and F is the parcel's area in m^2. In order to make a comparison, tolerance limit values (df_{max}) of parcel areas were calculated according to Eq. 9 and compared with the absolute $|dF|$ values found in this study. Accordingly, $|dF|$ values were obtained below the tolerance limit (df_{max}) in 1329 of 1333 parcels. In 4 parcels, the $|dF|$ value was greater than df_{max}. According to these results, 99.70% of the $|dF|$ values were lower than the tolerance limit (df_{max}) value specified in Eq. 9 given in the related the regulation. This shows that the earthquake effect did not cause significant changes on the areas.

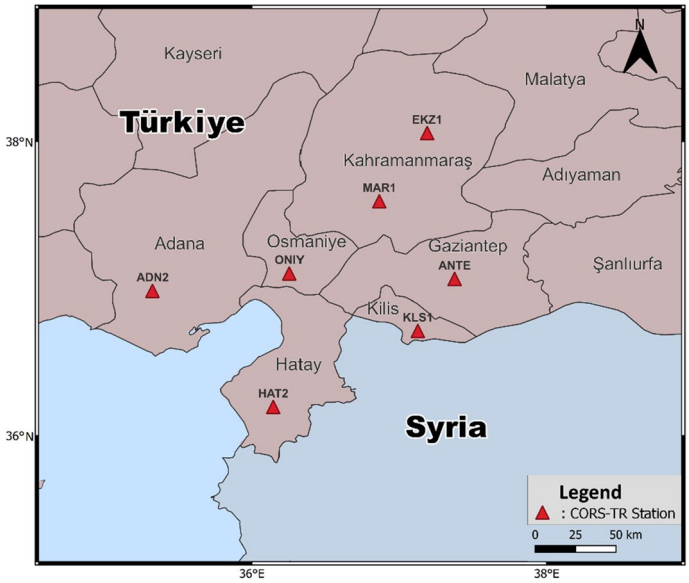


Fig. 10 Distribution of CORS-TR stations in the study area

Table 5 Velocities of CORS-TR stations in the study area (HGM 2023)

Station name	V_n (mm/year)	V_e (mm/year)	V_u (mm/year)
ADN2	17.45	13.32	− 1.92
ANTE	24.22	18.56	− 1.05
EKZ1	20.17	12.41	0.33
HAT2	21.15	18.36	1.06
KLS1	34.08	11.54	3.03
MAR1	20.45	14.64	− 1.26
ONIY	19.70	13.81	− 0.97

In a more general context, the North Anatolian and Southern Anatolian fault lines caused a horizontal displacement of up to 8 m in the 6 February earthquakes. This has destroyed infrastructure, roads, railways, and many buildings (Hussain et al. 2023). On the other hand, Liu et al. (2023) revealed that the maximum slip of both earthquakes reached about 10 m. According to Karabacak et al. (2023), the total fracture length in the Karasu, Pazarcık and Erkenek segments of the Eastern Anatolian Fault Zone is 270 ± 10 km, the left-lateral strike-slip faulting causes a maximum displacement of 7.30 m. They also state that although the surface rapture generally shows a narrow deformation zone width of 2–5 m, this width is up to 50 m in some parts of the faults.

Besides, independent from earthquakes, annual changes occur in point coordinates due to tectonic reasons in Türkiye. In this context, the distribution of CORS-TR stations in the region prepared in (QGIS.org 2023) is shown in Fig. 10 and the point velocities of the stations are shown in Table 5 (HGM 2023). When the data in the table is examined, it is seen that there is an annual change of 17.45–34.08 mm in the north direction,

11.54–18.56 mm in the east direction, and − 1.92–3.03 mm in the up direction in the point coordinates according to the ITRF solutions around the study area. Hence, it can be seen from the Table (5) that all points in the region move due to tectonic activities even if there is no earthquake occurring.

6 Conclusions

The earth we live on is significantly affected by natural disasters such as earthquakes, storms, floods, landslides, and tsunamis. Especially due to large earthquakes, surface deformations occur in the earth's crust. Even in the absence of an earthquake, certain magnitudes of changes are observed in point coordinates over time due to tectonic plate movements. Continuous determination of these changes caused by earthquakes and other natural events in order to ensure the continuity of the country's cadastral system and property data in an up-to-date and correct manner. In Türkiye, it is important in the context of the protection of the right to property, which is guaranteed by the constitution.

With this study, it has been tried to determine the changes in the cadastral and property data of the region due to the earthquakes in Kahramanmaraş and Hatay in Türkiye. For this purpose, the post-earthquake coordinates of the points whose pre-earthquake coordinates are known with high accuracy in Kırıkhan district of Hatay province were measured. By using the coordinates before and after the earthquake, the displacement amounts in the study area were modeled. With the help of the obtained model, the changes in the cadastral and property data were determined. Accordingly, position changes of up to 2.015 m in the north direction and up to 0.498 m in the east direction were detected at the points in the study area. According to these results, when examining the effects of earthquakes on cadastral parcels, it is considered that it would be a suitable method to consider coordinate changes instead of area changes when updating property data due to earthquakes, since area changes are generally smaller than 1 m^2. It would be more accurate to recalculate the parcel area values over these updated coordinates. In this study, the research has been tried to be discussed generally only from a geodetic perspective in order to contribute cadastre works. On the other hand, we know that for institutions performing cadastre, procedures are carried out by also taking into account the area and neighborhood relations of the parcels. For this reason, recalculated parcel area values were also evaluated with the parcel area tolerance limit values calculated by Eq. (9). Moreover, as a result of the studies and findings, it is seen that it is necessary to update the cadastral data due to earthquakes and to take into account the time dimension (change over time) in the coordinates regardless of earthquakes.

Acknowledgements We would like to thank the staff and collaborators of the General Directorate of Land Registry and Cadastre for providing the data used in this study and performing the land measurements.

Author contributions E. Tuşat, M. Aslan and C. Taşpınar contributed to data collection; E. Ayso, E. Tuşat, S. Doğanalp, M. Kahveci and İ. Köz processed the experimental data, performed the analysis, and drafted the manuscript; E. Ayso and İ. Köz designed the figures. All authors discussed the results and commented on the manuscript and all authors contributed to writing the manuscript.

Funding Open access funding provided by the Scientific and Technological Research Council of Türkiye (TÜBİTAK). The authors have not disclosed any funding.

Declarations

Conflict of interest The authors have not disclosed any competing interests.

Open Access This article is licensed under a Creative Commons Attribution 4.0 International License, which permits use, sharing, adaptation, distribution and reproduction in any medium or format, as long as you give appropriate credit to the original author(s) and the source, provide a link to the Creative Commons licence, and indicate if changes were made. The images or other third party material in this article are included in the article's Creative Commons licence, unless indicated otherwise in a credit line to the material. If material is not included in the article's Creative Commons licence and your intended use is not permitted by statutory regulation or exceeds the permitted use, you will need to obtain permission directly from the copyright holder. To view a copy of this licence, visit http://creativecommons.org/licenses/by/4.0/.

References

AFAD (2023a) Türkiye Deprem Tehlike Haritası. https://www.afad.gov.tr/turkiye-deprem-tehlike-haritasi Accessed 20 Jul 2023.

AFAD (2023b) Earthquake Catalog. https://deprem.afad.gov.tr/event-catalog Accessed 07 Aug 2023.

AFAD (2023c) 06 Şubat 2023 Pazarcık (Kahramanmaraş) Mw 7.7 Elbistan (Kahramanmaraş) Mw 7.6 Depremlerine İlişkin Ön Değerlendirme Raporu. Deprem Dairesi Başkanlığı. https://deprem.afad.gov.tr/assets/pdf/Kahramanmaras%20%20Depremleri_%20On%20Degerlendirme%20Raporu.pdf Accessed 20 Jul 2023

AFAD (2023d) 20 Şubat 2023 Yayladağı (Hatay) Mw 6.4 Depremine İlişkin Ön Değerlendirme Raporu. Deprem Dairesi Başkanlığı. https://deprem.afad.gov.tr/assets/pdf/Yayladağı%20(Hatay)%20Depremi%20MW%206.4%20Ön%20Degerlendirme%20Raporu.pdf Accessed 20 Jul 2023

Anadolu Ajansı (2023) Gündem Asrın Felaketi. https://www.aa.com.tr/tr/asrin-felaketi/kahramanmaras-merkezli-depremlerde-hayatini-kaybedenlerin-sayisi-50-bin-96-oldu/2850716 Accessed 07 Aug 2023.

Akaike H (1973) Information theory as an extension of the maximum likelihood principle. In: Petrov BN, Caski F (eds) Second international symposium on information theory. Akademiai Kiado, Budapest, pp 267–281

Altamimi Z, Métivier L, Rebischung P, Rouby H, Collilieux X (2017) ITRF2014 plate motion model. Geophys J Int 209(3):1906–1912. https://doi.org/10.1093/gji/ggx136

Anderson D, Burnham K (2004) Model selection and multi-model inference. Second NY: Springer-Verlag 63(2020):10

Aslan M (2023) Deprem ve Kadastro. Tapu Kadastro Mülkiyet, https://tkgmmakale.com/deprem-ve-kadastro Accessed 20 Jul 2023.

Aydogdu HH, Ilki A (2024) Case study for a performance based rapid seismic assessment methodology (PERA2019) based on actual earthquake damages. Bull Earthq Eng 22(2):1–35

Barra AF, Torhonen MP, Rajabifard A, Potts K, Grover RJ (2020) Solid ground: increasing community resilience through improved land administration and geospatial information systems

Biricik AS, Korkmaz S (2001) Kahramanmaraş'ın Depremselliği. Marmara Coğrafya Dergisi 3(1):53–82

Boğaziçi University Kandilli Observatory and Earthquake Research Instıtute Regional Earthquake-Tsunami Monitoring Center (BOUN KOERI RETMC) (2023) http://www.koeri.boun.edu.tr/sismo/2/son-depremler/harita-uzerinde/ Accessed 24 Jul 2023.

BÖHHBÜY (2005) Large Scale Map and Map Information roduction Regulation. Off Gazette Dated 23(06):2005

BÖHHBÜY (2018) Large scale map and map information roduction regulation. Off Gazette Dated 30(04):2018

Camargo AP, Sentelhas PC (1997) Performance evaluation of different potential evapotranspiration estimating methods in the state of São Paulo, Brazil. Rev Brasileira Agrometeorol 5:89–97

Cavanaugh JE, Neath AA (2019) The Akaike information criterion: Background, derivation, properties, application, interpretation, and refinements. Wiley Interdiscip Rev Comput Stat 11(3):e1460. https://doi.org/10.1002/wics.1460

T.R. Constitution, Türkiye Cumhuriyeti Anayasası (1982) Madde 35. RG, 09 Kasım 1982, Sayı 17863 (Mükerrer).

Dale PF, McLaughlin JD (1988) Land information management: an introduction with special reference to cadastral problems in Third World countries. Oxford University Press

Ercan O (2023) Evolution of the cadastre renewal understanding in Türkiye: A fit-for-purpose renewal model proposal, Land Use Policy, Volume 131, August 2023, 106755, https://doi.org/10.1016/j.landusepol.2023.106755

ESRI (2023) ArcGIS Pro Desktop: Release 10. Redlands, CA: Environmental Systems Research Institute. Accessed 20 July 2023

FIG (1995) Statement on Cadastre, Publication No. 11, Fédération Internationale des Géomètres, https://www.fig.net/organisation/comm/7/Library/reports/cadastre/statement_on_cadastre.html Accessed 20 July 2023.

GDLRC (2012) Digitization of Cadastre Maps, Article 14, Circular No: 1737 (2012/15).

Grant D, Crook C (2012) Spatial maintenance of the New Zealand cadastre in response to earthquakes. Proceedings of FIG Working Week, Rome, Italy.

Grant D, Crook C, Donnelly N (2014) Managing the Dynamics of the New Zealand spatial cadastre. Proceedings of Research, Canberra, Australia. pp. 60–71

Hay WW (1996) Tectonics and climate. Geol Rundschau 85:409–437

HGM (2023). TUSAGA-Aktif istasyonlarına ait hızlar, https://www.harita.gov.tr/public/sunum/, Accessed 10 Aug 2023.

Hua J, Fischer KM, Becker TW, Gazel E, Hirth G (2023) Asthenospheric low-velocitty zone consistent with globally prevalent partial melting. Nat Geosci 16:175–181

Hussain E, Kalaycıoğlu S, Milliner CW, Çakir Z (2023) Preconditioning the 2023 Kahramanmaraş (Türkiye) earthquake disaster. Nat Rev Earth Environ 4(5):287–289. https://doi.org/10.1038/s43017-023-00411-2

Jagoda M (2021) Determination of motion parameters of selected major tectonic plates based on GNSS station positions and velocities in the ITRF2014. Sensors 21(16):5342. https://doi.org/10.3390/s21165342

Jang JS (1993) ANFIS: adaptive-network-based fuzzy inference system. IEEE Trans Sys Cybern 23(3):665–685. https://doi.org/10.1109/21.256541

Jang JS, Sun CT (1995) Neuro-fuzzy modeling and control. Proceed IEEE 83(3):378–406. https://doi.org/10.1109/5.364486

Kahveci M, Yıldız F (2022) GPS/GNSS Uydularla konum belirleme sistemleri (GNSS): teori ve uygulama, 11. Basım, Nobel Yayıncılık, Ankara

Kahveci M, Çırmık A, Doğru F, Pamukçu O, Gönenç T (2019) Subdividing the tectonic elements of aegean and eastern mediterranean with gravity and GPS data. Solid Earth Sci 67:491–500. https://doi.org/10.1007/s11600-019-00270-w

Karabacak V, Özkaymak Ç, Sözbilir H, Tatar O, Aktuğ B, Özdağ ÖC, Çakir R, Aksoy E, Koçbulut F, Softa M, Akgün E, Demir A, Arslan G (2023) The 2023 Pazarcık (Kahramanmaraş, Türkiye) earthquake (Mw 7.7): implications for surface rupture dynamics along the east anatolian fault zone. J Geol Soc 180(3):jgs2023–jgs3020

Karaboga D, Kaya E (2019) Adaptive network based fuzzy inference system (ANFIS) training approaches: a comprehensive survey. Artif Intell Rev 52:2263–2293. https://doi.org/10.1007/s10462-017-9610-2

Kincey ME, Rosser NJ, Densmore AL, Robinson TR, Shrestha R, Singh Pujara D, Horton P, Swirad TR, Oven KJ, Arrell K (2023) Modelling post-earthquake cascading hazards: changing patterns of landslide runout following the 2015 Gorkha earthquake Nepal. Earth Surf Process Landf 48(3):537–554. https://doi.org/10.1002/esp.5501

Kop A, Ezer M, Bodur MN, Darbaş G, Inan S, Ergintav S, Seyis C, Yalçin C (2014) Geochemical monitoring along the Türkoğlu (Kahramanmaraş)-Gölbaşı (Adıyaman) segments of the east anatolian fault system. Arab J Sci Eng 39:5521–5536. https://doi.org/10.1007/s13369-013-0912-7

Koyanagi K, Gomi T, Sidle RC (2020) Characteristics of landslides in forests and grasslands triggered by the 2016 Kumamoto earthquake. Earth Surf Process Landf 45:893–904. https://doi.org/10.1002/esp.4781

Kurt Aİ, Özbakır AD, Cingöz A, Ergintav S, Doğan U, Özarpacı S (2022) Contemporary velocity field for Türkiye inferred from combination of a dense network of long term GNSS observations. Turkish Journal of Earth Sciences, 31. https://doi.org/10.55730/1300-0985.1844

Liu J, Li X, Nobile A, Klinger Y, Jónsson S (2023) Fault slip and fault-zone damage of the 6 February 2023 Kahramanmaraş earthquake duplet estimated from 3D displacement derivations of Sentinel-1 radar images (No. EGU23-17611). Copernicus Meetings. https://doi.org/10.5194/egusphere-egu23-17611

Mitchell D, Grant D, Roberge D, Bhatta GP, Caceres C (2017) An evalutation framework for earthquake-responsive land administration. Land Use Policy 67:239–252. https://doi.org/10.1016/j.landusepol.2017.05.020

Pal SC, Saha A, Chowdhuri I, Ruidas D, Chakrabortty R, Roy P, Shit M (2023) Earthquake hotspot and coldspot: Where, why and how? Geosys Geoenviron 2(1):100130. https://doi.org/10.1016/j.geogeo.2022.100130

Park JH, Park SH, Kim KA (2019) Disaster management and land administration in South Korea: Earthquakes and real estate market. Land Use Policy 85:52–62. https://doi.org/10.1016/j.landusepol.2019.03.040

QGIS.org, (%2023) QGIS Geographic Information System. QGIS Association. http://www.qgis.org Accessed 20 Jul 2023.

Ramstein G, Godderis Y, Donnadieu Y, Sepulchre P, Fluteau F, Zhang Z, Zhang R, Su B, Jiang D, Schuster M, Besse J (2019) Some illustrations of large tectonically driven climate changes in earth history. Tectonics 38:4454–4464. https://doi.org/10.1029/2019TC005569

Sagbas G, Sheikhi Garjan R, Sarikaya K, Deniz D (2024) Field reconnaissance on seismic performance and functionality of Turkish industrial facilities affected by the 2023 Kahramanmaras earthquake sequence. Bull Earthq Eng 22(1):227–254. https://doi.org/10.1007/s10518-023-01741-8

Sugeno M, Kang GT (1988) Structure identification of fuzzy model. Fuzzy Sets Sys 28(1):15–33. https://doi.org/10.1016/0165-0114(88)90113-3

Sünbül F, Sünbül AB (2017) Deprem Etkileşimlerinde Coulomb Gerilme Kriteri Değerlendirmesi; Doğu Anadolu Fay Hattı. Karaelmas Fen Ve Mühendislik Dergisi 8(2):523–535

Takagi T, Sugeno M (1985) Fuzzy identification of systems and its applications to modeling and control. IEEE Trans Sys Cybern 1:116–132. https://doi.org/10.1109/TSMC.1985.6313399

The MathWorks Inc (2020) MATLAB, version (R2020a), Natick, Massachusetts: The MathWorks Inc.. https://www.mathworks.com Accessed 20 Jul 2023

Tusat E, Mikailsoy F (2018) An investigation of the criteria used to select the polynomial models employed in local GNSS/leveling geoid determination studies. Arab J Geosci 11:1–15. https://doi.org/10.1007/s12517-018-4176-0

USGS (2023b) The United States geological survey. Ring of Fire. https://www.usgs.gov/media/images/ringoffiregif#:~:text=The%20"Ring%20of%20Fire"%2C,the%20world%27s%20earthquakes%20occur%20there Accessed 20 Jul 2023.

USGS (2023a) The United States geological survey. https://www.usgs.gov/faqs/where-do-earthquakes-occur Accessed 20 Jul 2023.

Willmott CJ (1981) On the validation of models. Phys Geogr 2(2):184–194. https://doi.org/10.1080/02723646.1981.10642213

Zadeh LA (1965) Fuzzy sets. Inf Control 8(3):338–353. https://doi.org/10.1016/S0019-9958(65)90241-X

Publisher's Note Springer Nature remains neutral with regard to jurisdictional claims in published maps and institutional affiliations.

Authors and Affiliations

Emre Ayso[1] · İrem Köz[1] · Serkan Doğanalp[1] · Mustafa Aslan[2] · Ekrem Tuşat[1] · Muzaffer Kahveci[1] · Cahit Taşpınar[3]

✉ Emre Ayso
eayso@ktun.edu.tr

İrem Köz
ikoz@ktun.edu.tr

Serkan Doğanalp
sdoganalp@ktun.edu.tr

Mustafa Aslan
maslan@tkgm.gov.tr

Ekrem Tuşat
etusat@ktun.edu.tr

Muzaffer Kahveci
mkahveci@ktun.edu.tr

Cahit Taşpınar
cahittaspinar@gmail.com

[1] Department of Geomatics Engineering, Faculty of Engineering and Natural Sciences, Konya Technical University, Konya, Turkey

[2] Cadastre Department, General Directorate of Land Registry and Cadastre, Ankara, Turkey

[3] Konya Regional Directorate, General Directorate of Land Registry and Cadastre, Konya, Turkey